



Experimental study of air–water up-flow in a packed column using laser Doppler anemometry

Y.S. Hernández-Demesa^a, C.A. Varela-Boydo^a, F.Z. Sierra-Espinosa^b,
L.F. Ramírez-Verduzco^c, J.L. Cano-Domínguez^c, J.A. Hernández^{b,c,*}

^aPosgrado en Ingeniería y Ciencias Aplicadas del Centro de Investigación en Ingeniería y Ciencias Aplicadas (CIICAp) de la Universidad Autónoma del Estado de Morelos (UAEM), Av. Universidad 1001, Col. Chamilpa, C.P. 62209, Cuernavaca, Morelos, Mexico

^bCentro de Investigación en Ingeniería y Ciencias Aplicadas (CIICAp) de la Universidad Autónoma del Estado de Morelos (UAEM), Av. Universidad 1001, Col. Chamilpa, C.P. 62209, Cuernavaca, Morelos, Mexico, Tel./Fax: +52 777 329 7084; email: alfredo@uaem.mx (J.A. Hernández)

^cProcesos de Transformación, Instituto Mexicano del Petróleo, Eje Central Norte Lázaro Cárdenas 152, C.P. 07730, México, DF, Mexico

Received 26 February 2014; Accepted 16 June 2014

ABSTRACT

The hydrodynamics of an air–water flow in a column has been analyzed. The reactor consisted of a vertical column of 0.055 m diameter and 0.255 m height, made of acrylic to achieve good visualization of the bubbles. The column was partially packed with solid cylindrical pellets. The study was focused on the region above the packed zone in three vertical positions. Measurements of velocity in ascendant flow direction were conducted at each position using laser Doppler anemometry. Velocities along the column diameter were experimentally determined for two liquids flow, 300 and 600 L/h. Two conditions of Reynolds number were obtained, $Re: 8.3$ and 16.7×10^3 based on inlet pipe diameter and water properties. The results show that the size and shape of the bubbles become smaller and uniform when the column was packed. Experimental measurements of the velocity were difficult to determine when the Re was higher ($Re > 17 \times 10^3$). Also, the velocity profile showed instability of the flow, mainly in the near packed region. However, an average value of the velocity could be observed as function of the inlet condition.

Keywords: Bubble column; Laser Doppler anemometry; Multiphase flow

1. Introduction

The bubble column reactors are commonly used in many areas of engineering, such as chemical, petro-

chemical, biology, biochemistry, pharmaceutical, and metallurgical industries, to name a few, in a variety of processes: hydrogenation, oxidation, chlorination, alkylation, effluent treatment, antibiotic, fermentation, bio-desulfurization of oil, etc. [1–8]. In particular, in the chemical industry, the Fischer–Tropsch process

*Corresponding author.

Presented at the Conference on Desalination for the Environment: Clean Water and Energy 11–15 May 2014, Limassol, Cyprus

(bubble column-type reactor) is widely used and known for the synthesis of methanol and fuels [9–21].

Although the geometry of the bubble column reactors is simple, the study of which is often complicated since these reactors use multiphase flows. Therefore, the design and scale-up of bubble columns depend upon the column hydrodynamics [5,22]. The most important parameters to achieve an optimal design of such reactors are: column dimensions, internal conditions, distribution of inlet flows, gas–liquid dispersion, operating conditions (T, P), physical and chemical properties of phases, size and structure of solid particles, and chemical reaction, among others. Involved physical phenomena to be investigated in bubble column reactors are: physical properties of bubbles, interfacial properties, momentum, heat and mass transfer, mixing, and the drop pressure, etc. The current design of a bubble column reactor is closer to empiricism based on the fundamental understanding of the hydrodynamic parameters [22]. Rzehak and Krepper [23] mentioned that the bubble in the fluid induces turbulent dissipation which affects the flow properties. Therefore, the hydrodynamic on packed reactors is influenced by the amount, size, and distribution of bubbles.

The study of the hydrodynamic behavior of packed columns depends on the use of experimental techniques such as Particle Image Velocimetry, Laser Doppler Anemometry (LDA), and Phase Doppler Anemometry (PDA) [24,25]. Gan et al. [26] examined the dynamic flow and stability of a two-phase bubbly cylindrical column with the PDA technique. The bubbles diameters were in the range of 400–1,300 μm . Measurements were taken at different air flow rates (0.13, 0.25, and 0.38 L/min) that correspond to the following gas volume fractions, 0.0065, 0.0138, and 0.0197. The authors found a pattern of constant circulation in the top of the column and instability of low frequency in the bottom of the column caused by bubbling. They recognized that the size of bubbles has an effect on the turbulence within the column. Braeske et al. [27] and Lain et al. [28] used PDA techniques to determine the phases hold-up in a bubble reactor. Magaud et al. [29] mentioned that decreasing the liquid velocity, considerably amplifies the gas velocity effect. The packed column reactors with co-current liquid–gas flows where heterogeneous reactions take place on solid surfaces are also applied to catalytic processes in refineries such as hydrocracking and hydrotreating processes. The lack of knowledge about proper distribution and dispersion of liquid and gas, optimum heat transfer, and reliable kinetic models can cause the reactor performance to decrease [1]. Consequently, the hydrodynamic study in this is crucial for reaching the optimum performance.

Therefore, the objective of this paper is to analyze the hydrodynamics of gas–liquid flow in a packed bubble column with cylindrical non-porous solids by using the LDA. The design and construction of the acrylic experimental device was carried out at laboratory scale. The packed column was operated with water and air. The LDA technique was used focusing laser beams in three vertical locations of the column, near to the border of the bed, in order to monitor the bubble velocity.

2. Experimental design of the packed column

An acrylic column (see Fig. 1) was made using 0.055 m diameter and 0.255 m height; the column length occupied by the solid phase was 0.16 m. The solid phase consists of non-porous cylindrical pellets of 316 stainless steel with an average dimension of 0.01 m length and 0.002 m diameter. The pellets occupy 23.8% of the column volume, leaving the rest for free circulation of fluids (see Fig. 2). The air and water were pumped through two separate lines that meet at the bottom of the experimental device where fluids were mixed. Steel waste debris was placed before the inlet of column in order to ensure a uniform air distribution in water showing good results. Likewise, the reactor has two outlets; one oriented horizontally that allows the output of most of the water, which is located after the packed zone; and the other on the top that directs the flow vertically towards a closed loop, as shown in Fig. 1. Two flowmeters with an accuracy of $\pm 1\%$ for water and $\pm 2\%$ for air were used in order to control the flow of both fluids. The pipe lines were equipped with two valves: a gate type for the water line and a needle type for the air line. Water was circulated in a closed loop using a submersible pump 1/8 hp, whereas the air was taken from the environment with a compressor 1 hp which was operated with a stationary *by-pass* in order to fix the pressure at the base of the column.

3. Experimental procedure

The hydrodynamic analysis of the column is based on measurements of velocity at three vertical coordinates located along the column at 0.208, 0.198, and 0.188 m. Measurements were carried out at points in the cross-sections by moving the laser beam horizontally from wall to wall and obtain the velocity profile. All measurements were conducted below the horizontal outlet of the column (see Fig. 3). Silver dioxide particles with an average size of 5 microns were used as markers of the bubble flow. In LDA, the velocity is



Fig. 1. Multiphase experimental system.

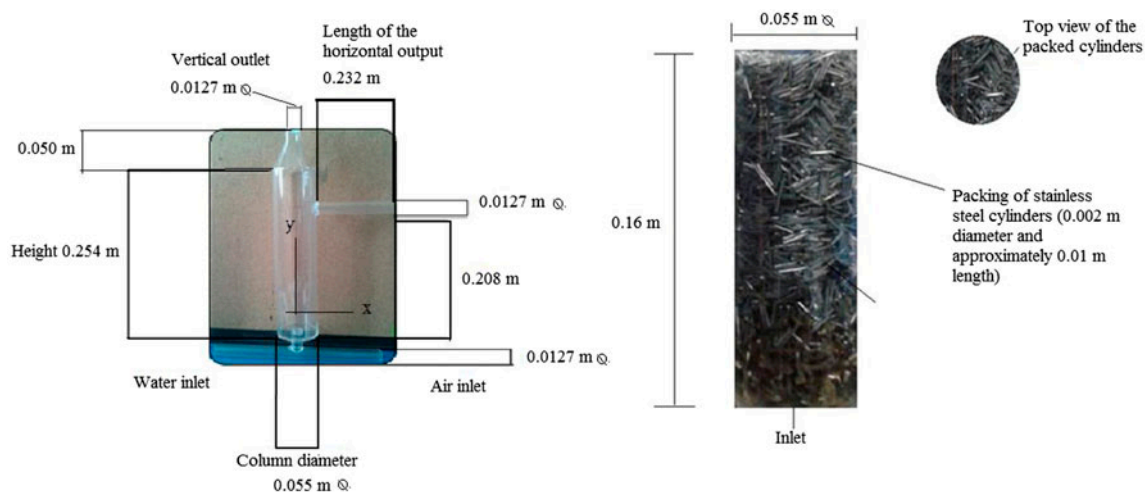


Fig. 2. Bubble column dimensions.

derived from Doppler frequency of marked particles that are illuminated by a known frequency of laser light when cross a fixed fringe, resulting from interaction of two laser beams in a small space called measurement volume, which is characterized by an interference fringes (a pattern of light and dark surface) [30].

When the marked particles pass through the illuminated zone, emit light pulses that are captured by a photodiode. These signals have a defined frequency from which the velocity is derived. This is possible

because the light scattered by the particle is collected by a front lens and focused on the photodetector which converts the fluctuations of light intensity into a voltage signal, which is in turn amplified. An electronic device known as signal processor is used to determine the frequency of each particle crossing the measurement volume.

The equation that relates the Doppler frequency, f_D , of the particle and its velocity, u_y , is deduced using physical considerations of laser light and optics geometry [31,32]:

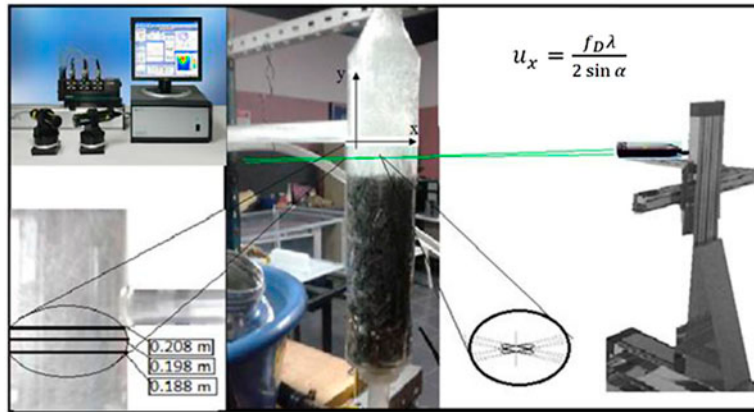


Fig. 3. Bubble column and anemometer used to determine the velocity of bubbles at the following vertical coordinates: 0.188, 0.198, and 0.208 m.

$$u_y = \frac{f_D \lambda}{2 \sin \alpha} \quad (1)$$

where f_D is the Doppler frequency in Hz; α is the beam angle; λ is the wavelength of the laser radiation (in this case, green color of 514 nm was used), and u_y is the velocity component in the plane formed by the laser beams, in m/s. In this study both laser beams were introduced aligned with the main axis of the column giving the component of the surface velocity in the vertical direction, u_y .

The results are plotted as velocity as a function of the distance in the x direction, which represents the column diameter (see Fig. 3). It is noteworthy that the gas and liquid velocities could not be measured by the LDA technique in the packed zone of the column, because the solid elements blocked the passage of light beams. It is important to mention that each measurement point by the LDA consists of over 1,500 burst data enabling a point velocities fluctuations description along the diameter of the column (see Fig. 3), except for the region close to the wall where a few number of data were obtained.

Table 1 shows the inlet conditions under study. Liquid flow rates of 300 and 600 L/h were mixed with

Table 1
Input conditions used to water and air

Flow rate (L/h)		Velocity (m/s)		Reynolds number		Re _a Two-phase
Water	Air	Water	Air	Water	Air	
300	54.5	0.66	0.12	8,329	108	656
600	54.5	1.32	0.12	16,659	108	1,312

a constant air flow of 54.5 L/h. Reynolds number was calculated based on the internal diameter of the inlet pipe and inlet velocity, before water and air were mixed. Additionally, packed beds Reynolds numbers were calculated according to Baker [33] (see Re_a Table 1).

4. Results and discussions

The system under study consisted of three phases: a static solid phase formed by cylindrical elements of stainless steel 316, a liquid phase (continuous phase) represented by water, and a gas phase (dispersed phase) given by the air. Visualization of the air–water mixture is lost within the packed column zone with the LDA technique. During the experiment, the formation of vortices in the horizontal outlet of the column and wall was observed. The above behavior induces the turbulent dissipation of bubbles that causing changes in the internal energy and properties of the mixture, similar to that reported by other authors [24,34,35]. After the packed zone it was observed that air bubbles evenly move vertically to the top of the column. Furthermore, less bubbles moved homogeneously towards the horizontal outlet at the upper part of the column. Regarding the behavior of two-phase flow a vortex near the horizontal output was observed.

Fig. 4 shows the bubble pattern after the bed for the two flows studied.

4.1. Velocity profiles obtained using LDA

The measurement of velocity with LDA was more difficult as the Reynolds number, Re, increased. As mentioned above, more than 1,500 data was obtained

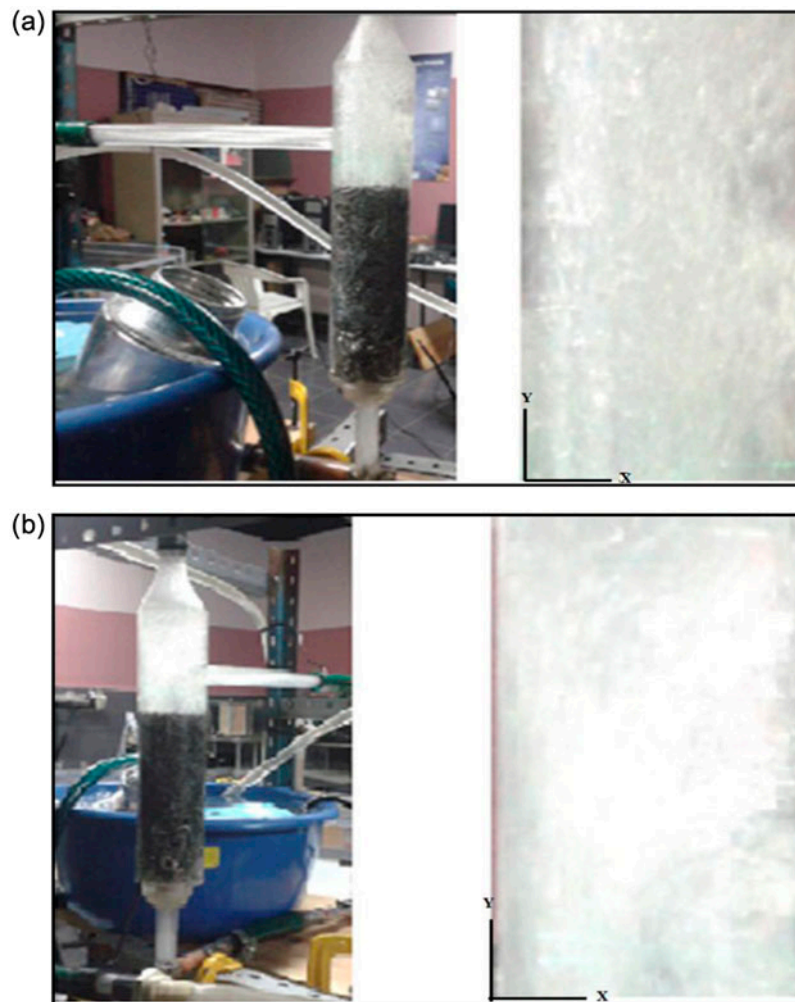


Fig. 4. Bubble pattern in column at (a) 300 L/h and (b) 600 L/h of water flow.

that were averaged for each experimental point being reported in this paper, which allow describing fluctuations on velocity along the column diameter, except near the wall, where a small number of data was obtained due to the erratic movement of the bubbles. The bubbles over there have a different dynamics compared with what occurs in the center zone of the column, as observed in Fig. 4(b).

Table 2 shows the average velocity for each position. As can be seen for the case of 600 L/h, the velocity increased as the fluid passed the solid phase and decreased as it moved away from the edge.

A summary of results is presented in Fig. 5, which shows the velocity profiles along the diameter of the column at three positions and water flow of 300 L/h. It is observed that velocity values disposed along the entire cross section showing large fluctuations. It is important to note that there are no measurements from wall to $x=0.01$ m (opposite the horizontal outlet).

Table 2
Experimental average velocity

Water flow rate (L/h)	Velocity (m/s)		
	Position (m)		
	0.188	0.198	0.208
300	0.124	0.138	0.147
600	0.251	0.24	0.239

The highest measured value of superficial velocity was 0.27 m/s located near the border to the solid border; this confirms a greater velocity when the fluid leaves the packed zone.

For the case of water flow of 600 L/h, the results are shown in Fig. 6. We can also confirm that high variation of velocity occurs near the walls of the column,

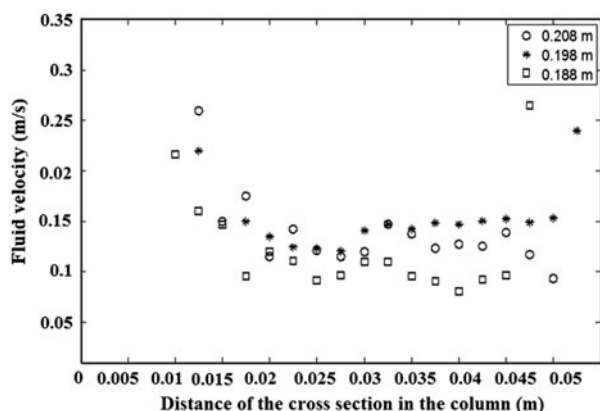


Fig. 5. Velocity profile along the cross section of the column measured at three vertical positions using 300 L/h of water and 54.5 L/h of air.

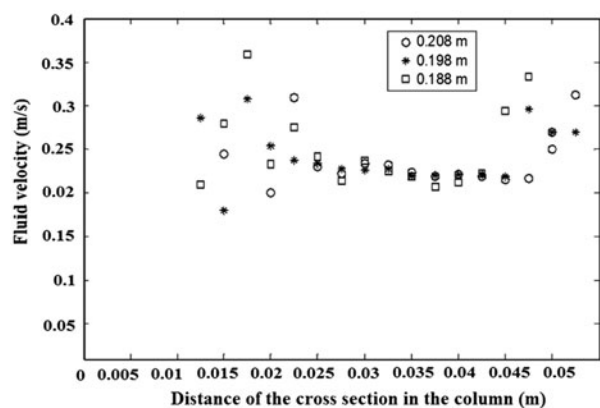


Fig. 6. Velocity profile along the cross section of the column measured at three vertical positions using 600 L/h of water and 54.5 L/h of air.

but unlike the results of Fig. 5, a similar region exists in the center with slightly higher velocity. This result indicates that the flow rate determined by the velocity profiles immediately after the packed column. Another important aspect is that measurements of velocity were possible after a distance of 0.01 m from the wall (opposed to the horizontal outlet). Similar to results of Fig. 5, the results in Fig. 6 show a highest velocity (0.36 m/s) close to the end of the packed column.

5. Conclusions

This work was focused on the experimental determination of velocity profiles in a packed bubble column using the LDA technique. The measurements were carried out at three vertical positions located near the package. Two inlet conditions for the water

flow were used (300 and 600 L/h), and keeping the air flow fixed at 54.5 L/h. In this case, Reynolds number was obtained for water inlet conditions of $Re = 8,329$ and $Re = 16,659$, while an air inlet condition of $Re = 90$ kept constant. The results showed high dispersion of velocity magnitude in the region above the solid cylindrical pellets (between 0.05 and 0.36 m/s). For the case of $Re = 8,329$ (300 L/h), a velocity of 0.27 m/s was reached while for the highest Re condition (600 L/h) a velocity of 0.36 m/s was achieved according to the measurement positions under study in this work. Compared with the inlet condition, the velocity of water was reduced due to the solid phase in the column.

The formation of vortices was evident both in the horizontal output and the column wall. Then, a greater velocity variation near to the solid phase (vertical coordinate) and wall (horizontal coordinate) was obtained. Pellets promoted the formation of small and uniform bubbles, as well as a regular water flow.

In the packed zone no velocity measurements were obtained because pellets obstructed the passage of light beams.

Acknowledgement

J.A. Hernández expresses his sincere gratitude to the “Instituto Mexicano del Petróleo” for the financial support received from a research stay.

References

- [1] M. Salimi, S. Hashemabadi, S. Noroozi, A. Heidari, M. Bazmi, Numerical and experimental study of catalyst loading and body effects on a gas–liquid trickle-flow bed, *Chem. Eng. Technol.* 36(1) (2013) 43–52.
- [2] T. Zhang, C. Wei, C. Feng, J. Zhu, A novel airlift reactor enhanced by funnel internals and hydrodynamics prediction by the CFD method, *Bioresour. Technol.* 104 (2012) 600–607.
- [3] C. Loha, H. Chattopadhyay, P.K. Chatterjee, Assessment of drag models in simulating bubbling fluidized bed hydrodynamics, *Chem. Eng. Sci.* 75 (2012) 400–407.
- [4] B. Ashraf Ali, S. Pushpavanam, Analysis of unsteady gas–liquid flows in a rectangular tank: Comparison of Euler–Eulerian and Euler–Lagrangian simulations, *Int. J. Multiphase Flow* 37(3) (2011) 268–277.
- [5] W. Bai, Experimental and Numerical Investigation of Bubble Column Reactors, Ipskamp Drukkers B.V., Enschede, 2010, ISBN: 978-90-386-2405-1.
- [6] N. Kantarci, F. Borak, K.O. Ulgen, Bubble column reactors, *Process Biochem.* 40(7) (2005) 2263–2283.
- [7] M.R. Mehrnia, B. Bonakdarpour, J. Towfighi, M.M. Akbarnejad, Design and operational aspects of airlift bioreactors for petroleum biodesulfurization, *Environ. Prog.* 23(3) (2004) 206–214.

- [8] M.M. Carbonell, R. Guirardello, Modelling of a slurry bubble column reactor applied to the hydroconversion of heavy oils, *Chem. Eng. Sci.* 52(21–22) (1997) 4179–4185.
- [9] S.C. Araujo-Ferrer, A. De Almeida, A. Zabala, A. Granados, Use of catalysts in Fischer–Tropsch process, *Revista Mexicana de Ingeniería Química* 12(2) (2013) 257–269.
- [10] J.M. Van Baten, R. Krishna, Eulerian simulation strategy for scaling up a bubble column slurry reactor for Fischer–Tropsch synthesis, *Ind. Eng. Chem. Res.* 43(16) (2004) 4483–4493.
- [11] G. Arzamendi, P.M. Diéguez, M. Montes, J.A. Odriozola, E. Falabella Sousa-Aguiar, L.M. Gandía, Computational fluid dynamics study of heat transfer in a microchannel reactor for low-temperature Fischer–Tropsch synthesis, *Chem. Eng. J.* 160(3) (2010) 915–922.
- [12] D.P. Guillen, T. Grimmitt, A.M. Gandrik, S.P. Antal, Development of a computational multiphase flow model for Fischer Tropsch synthesis in a slurry bubble column reactor, *Chem. Eng. J.* 176–177 (2011) 83–94.
- [13] B. Ashraf Ali, S. Pushpavanam, Experimental and computational investigation of two phase gas–liquid flows: Point source injection at the center, *Ind. Eng. Chem. Res.* 50(23) (2011) 13220–13229.
- [14] H. Ma, J. Xiao, B. Wang, Environmentally friendly efficient coupling of n-heptane by sulfated tri-component metal oxides in slurry bubble column reactor, *J. Hazard. Mater.* 166(2–3) (2009) 860–865.
- [15] T.A. Gauthier, Current R&D challenges for fluidized bed processes in the refining industry, *Int. J. Chem. Reactor Eng.* 7(1) (2009) 1–16.
- [16] A. Jess, C. Kern, Influence of particle size and single-tube diameter on thermal behavior of Fischer–Tropsch reactors: Part I: Particle size variation for constant tube size and vice versa, *Chem. Eng. Technol.* 35(2) (2012) 369–378.
- [17] A. Jess, C. Kern, Influence of particle size and single-tube diameter on thermal behavior of Fischer–Tropsch reactors: Part II: Eggshell catalysts and optimal reactor performance, *Chem. Eng. Technol.* 35(2) (2012) 379–386.
- [18] C. Hulet, P. Clement, P. Tochon, D. Schweich, N. Dromard, J. Anfray, Literature review on heat transfer in two and three-phase bubble columns, *Int. J. Chem. Reactor Eng.* 7 (2009) 1–94.
- [19] R. Guettel, U. Kunz, T. Turek, Reactors for Fischer–Tropsch synthesis, *Chem. Eng. Technol.* 31(5) (2008) 746–754.
- [20] A. Joelianingsih, H. Nabetani, Y. Sagara, A.H. Tambunan, K. Abdullah, A continuous-flow bubble column reactor for biodiesel production by non-catalytic transesterification, *Fuel* 96 (2012) 595–599.
- [21] L. Sehabiague, R. Lemoine, A. Behkish, Y.J. Heintz, M. Sanoja, R. Oukaci, B.I. Morsi, Modeling and optimization of a large-scale slurry bubble column reactor for producing 10,000 bbl/day of Fischer–Tropsch liquid hydrocarbons, *J. Chin. Inst. Chem. Eng.* 39(2) (2008) 169–179.
- [22] G.Q. Yang, B. Du, L.S. Fan, Bubble formation and dynamics in gas–liquid–solid fluidization: A review, *Chem. Eng. Sci.* 62(1–2) (2007) 2–27.
- [23] R. Rzehak, E. Krepper, CFD modeling of bubble-induced turbulence, *Int. J. Multiphase Flow* 55 (2013) 138–155.
- [24] L. Vázquez, A. Alvarez-Gallegos, F.Z. Sierra, C. Ponce de León, F.C. Walsh, Simulation of velocity profiles in a laboratory electrolyser using computational fluid dynamics, *Electrochim. Acta* 55 (2010) 3437–3445.
- [25] M.R. Bhole, S. Roy, J.B. Joshi, Laser doppler anemometer measurements in bubble column: Effect of sparger, *Ind. Eng. Chem. Res.* 45(26) (2006) 9201–9207.
- [26] Z.W. Gan, S.C.M. Yu, A.W.K. Law, Hydrodynamic stability of a bubble column with a bottom-mounted point air source, *Chem. Eng. Sci.* 66(21) (2011) 5338–5356.
- [27] H. Braeske, G. Brenn, J. Domnick, F. Durst, A. Melling, M. Zieme, Extended phase-doppler anemometry for measurements in three-phase flows, *Chem. Eng. Technol.* 21(5) (1998) 415–420.
- [28] S. Lain, D. Bröder, M. Sommerfeld, Experimental and numerical studies of the hydrodynamics in a bubble column, *Chem. Eng. Sci.* 54(21) (1999) 4913–4920.
- [29] F. Magaud, M. Souhar, G. Wild, N. Boisson, Experimental study of bubble column hydrodynamics, *Chem. Eng. Sci.* 56(15) (2001) 4597–4607.
- [30] Y. Yeh, H.Z. Cummins, Localized fluid flow measurements with an He–Ne laser spectrometer, *Appl. Phys. Lett.* 4(10) (1964) 176–178.
- [31] W.J. Devenport, *Laser Doppler Anemometry*, AOE 3054 Experimental Methods, Course Manual, 1995.
- [32] Dantec Dynamics, *Laser Doppler Anemometry: Introduction to Principles and Applications*, Dantec Dynamics, 2009. Internet consulted July 25, 2013. Available from: http://faculty.ksu.edu.sa/azzeer/Documents/534%20PHYS/LN7_LDA_s.pdf. Internet consulted July 25, 2013.
- [33] M. J. Baker, CFD simulation of flow through packed beds using the finite volume technique, PhD Thesis, University of Exeter, 2011.
- [34] L. Zhang, G. Cheng, S. Gao, Experimental study on air bubbling humidification, *Desalin. Water Treat.* 29(1–3) (2011) 258–263.
- [35] L. Zhang, W. Chen, H. Zhang, Study on variation laws of parameters in air bubbling humidification process, *Desalin. Water Treat.* 51(16–18) (2013) 3145–3152.